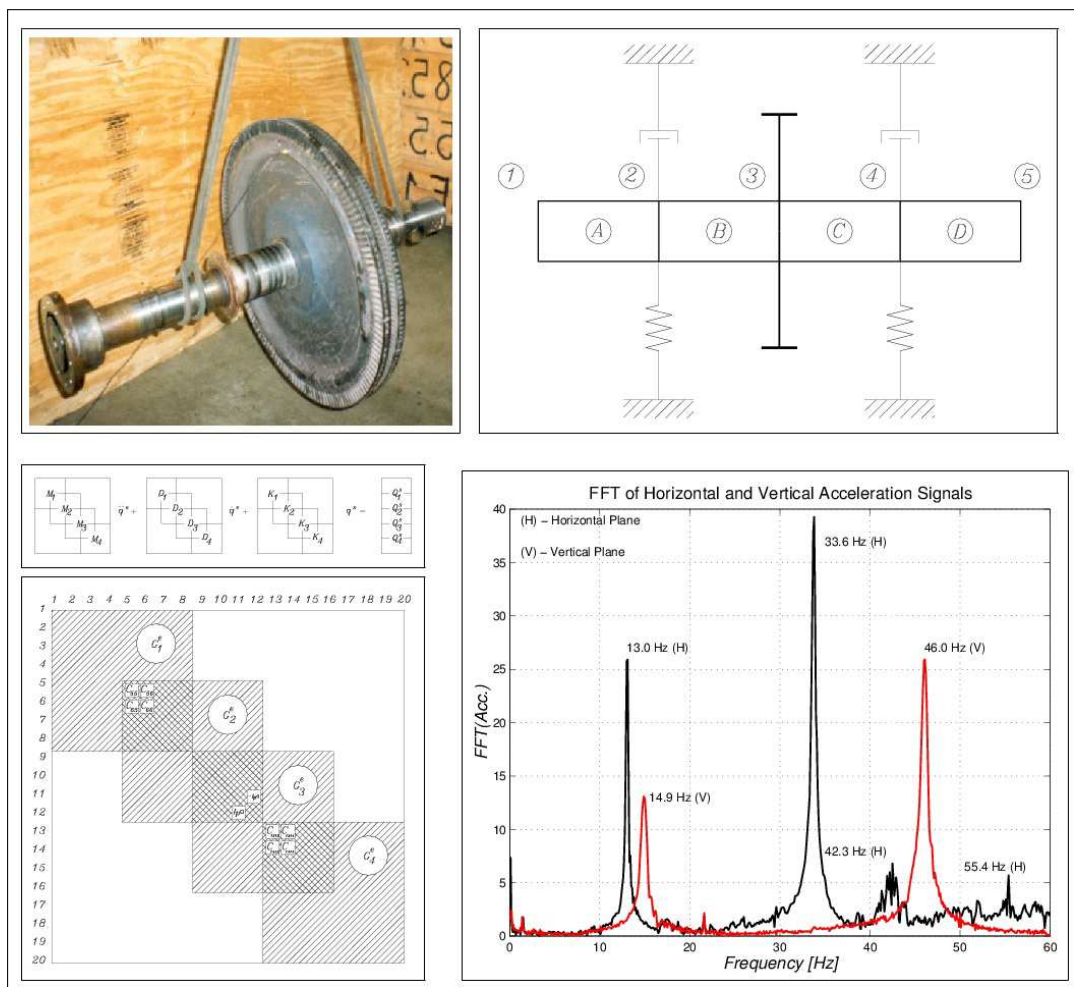


Project 2

– Dynamics of Rotor-Bearing Systems –

Lateral Vibrations and Stability Threshold of Flexible Rotors Supported On Hydrodynamic and Ball Bearings.



Ilmar Ferreira Santos, Prof. Dr.-Ing. dr. techn.

Section of Solid Mechanics

Department of Mechanical Engineering

Technical University of Denmark

2800 Lyngby, Denmark

e-mail: ifs@mek.dtu.dk

phone: +45 45256269

1 Introduction

The occurrence of instability in rotating machines is a very typical problem, especially in high-speed machines, and may be caused by fluid-structure interactions due to oil film forces presented in hydrodynamic bearings or aerodynamic forces resulting from seals, among others. A machine designer normally wants to know the range of angular velocity in which the machine will operate stable and without vibration problems, i.e. maximum angular velocity and distance from the unstable operational range.

This second project in the discipline aims to make you familiar with the prediction of critical speeds in rotating machines, stability threshold, and unbalance response and maximum vibration amplitude while crossing critical speed ranges.

Aiming at dealing with a real rotor-bearing problem, the test rig illustrated in figure 1(a) will be used as an example of a rotating machine. It will facilitate the visualization of the problem and aid the students to link the theoretical results to practical problems and experimental results. The test rig shown in figure 1(a) simulates a large overhung centrifugal compressor. The scheme of a large overhung centrifugal compressor can be seen in figure 1(b). The test rig, as well as the overhung centrifugal compressor, is composed of one flexible shaft and discs or impellers positioned at the end of the shaft. The shaft is laterally supported by two bearings. In the test rig, the bearing closest to the coupling will operate as thrust bearing as well. All technical information needed is given in this project description. By using all theoretical and experimental tools related to Rotor Dynamics obtained during the classes, you will win a solid overview and understanding of how real and imaginary parts of eigenvalues – and consequently also eigenvectors – change as a function of the operational speeds.

The steps of the project are summarized as follows:

- First, you have to obtain mechanical and mathematical models of the flexible shaft element using Finite Element Method (FEM).
- Second, the disc (impeller) shall be mounted onto the shaft. Mechanical and mathematical models shall be expanded to cope with the dynamics of the disc or discs.
- Third, partial data from experimental modal testing is delivered and should be used to validate and/or adjust the finite element models built by you. The experimental apparatus, as well as the shaft and shaft nodes, are shown in figure 2. Three testing configurations are used as illustrated in figures 2(a), (b), and (c). In figure 2(a) the flexible shaft is mounted in an almost free-free condition, in figure 2(b) a disc of 100 mm thickness is mounted on the shaft, and (c) two discs of 100 mm and 80 mm thickness, respectively, are mounted on the flexible shaft.
- Finally, the flexible shaft connected to the rigid disc is mounted onto a ball bearing and a journal bearing, as it is shown in figure 1(a). The eigenvalues and eigenvectors will be calculated for the global rotor-bearing-system. These calculations will serve as the basis for an elaborate analysis involving mode shape visualization and stability.

It is worth to mention that the experimental modal analysis is carried hanging the flexible shaft in an almost free-free condition, as illustrated in figure 2. One accelerometer (element **1**) and one impact hammer coupled with a force transducer attached to an aluminum head (element **2**) are used to laterally excite the shaft and access the lateral vibration response of several shaft nodes, illustrated in red. Acceleration response and impact force signals are filtered with a cut-off frequency of 3000 Hz and amplified using two signal amplifiers (elements **3** and **4**).

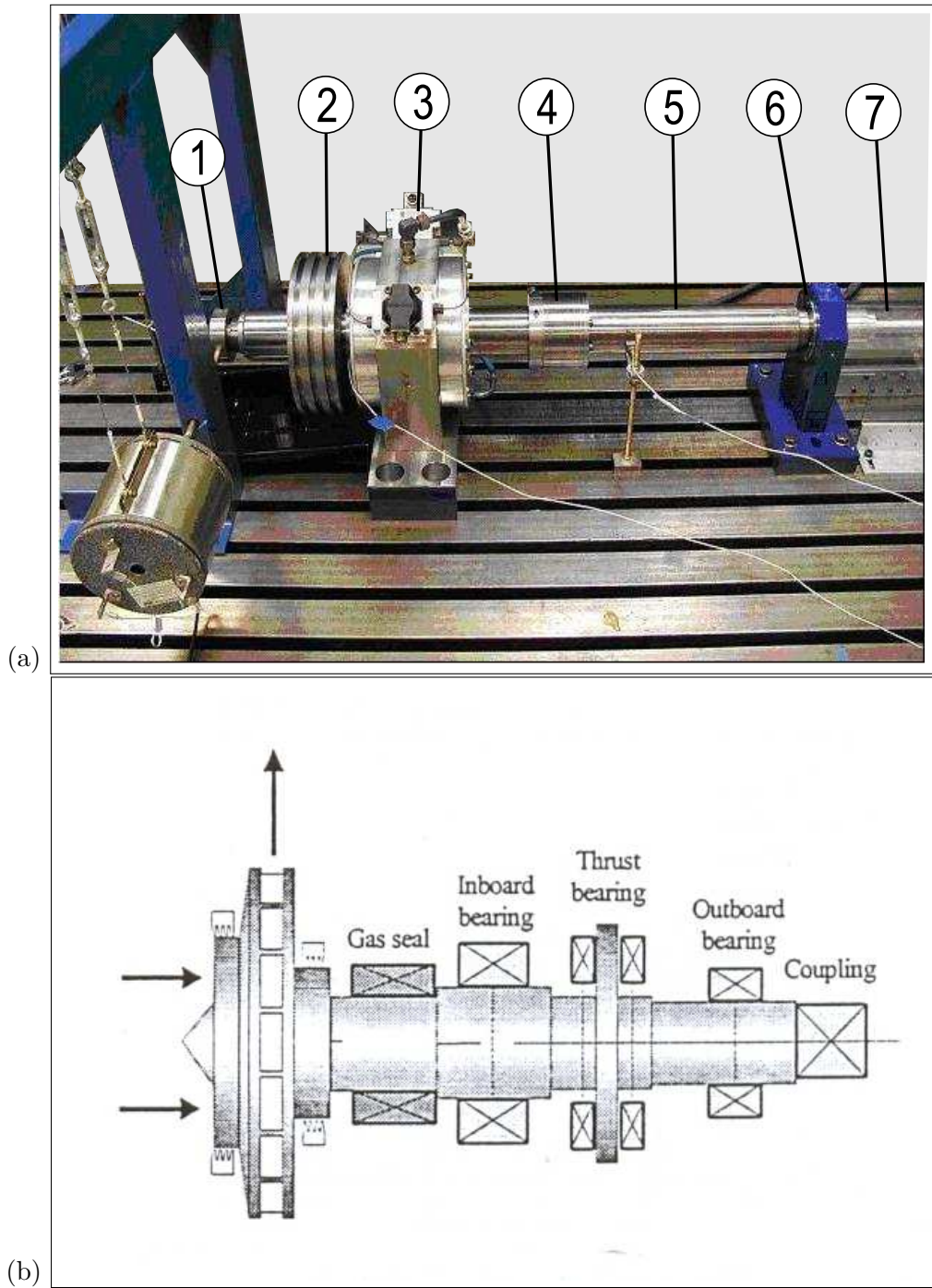


Figure 1: (a) Test rig built to simulate the dynamic behavior of an overhung centrifugal compressor; ①: Excitation point; ②: Disc; ③: Journal bearing; ④: Seal (neglect this component in the project); ⑤: Shaft; ⑥: Ball bearing (also functioning as thrust bearing); ⑦: Flexible coupling; (b) Operational scheme of a large overhung centrifugal compressor.

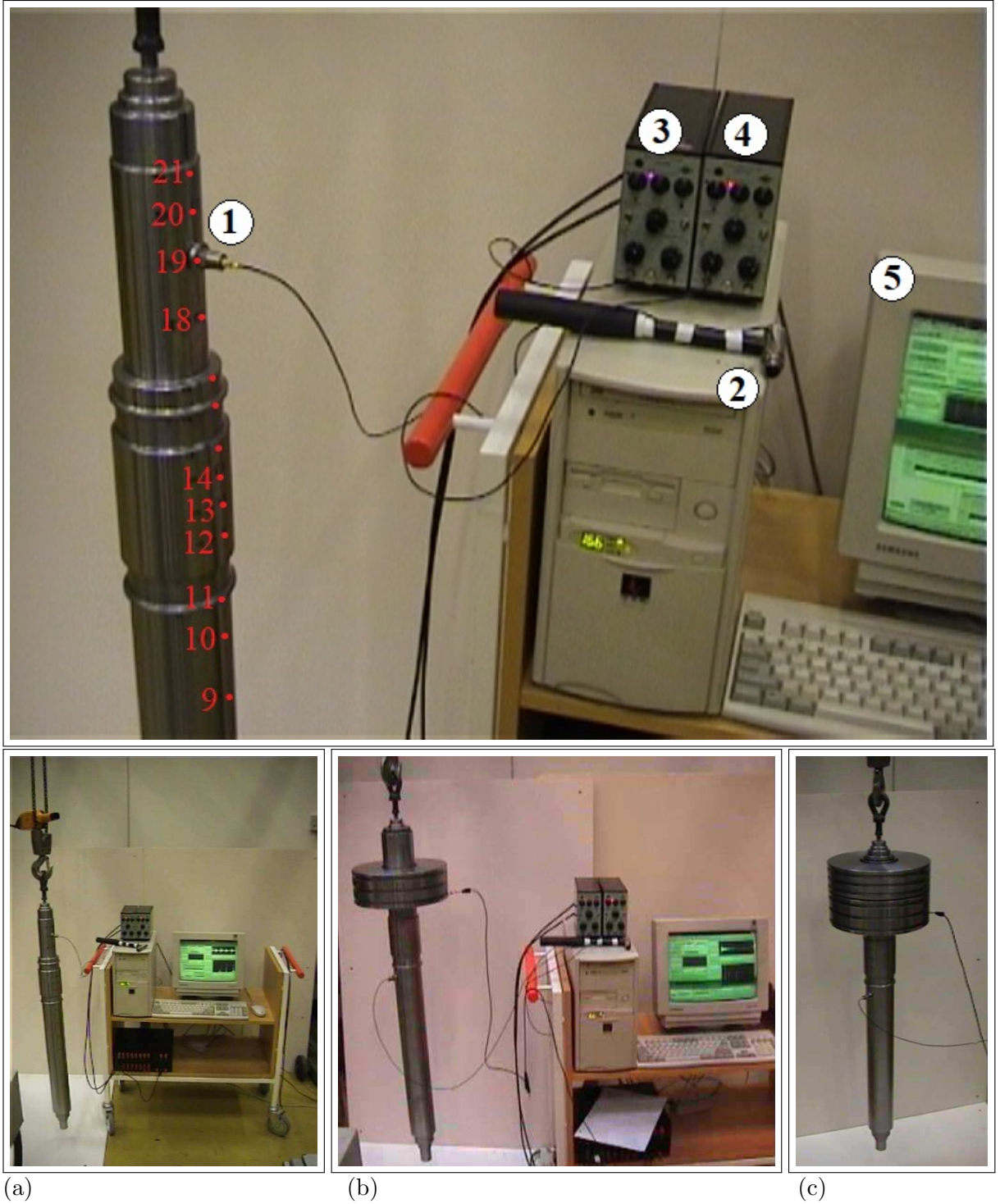


Figure 2: *Experimental modal testing of the flexible shaft in an almost free-free condition: accelerometer (element 1), hammer coupled with a force transducer attached to an aluminum head (element 2), two signal amplifiers (elements 3 and 4), and digital computer (element 5). (a) flexible shaft mounted in a free-free condition, (b) disc of 100 mm thickness mounted on the shaft, and (c) two discs of 100 mm and 80 mm thickness mounted on the flexible shaft.*

Both signals are simultaneously acquired by a digital computer (element 5) with an acquisition frequency of 6000 Hz and a time of 3 seconds. The test is performed using three configurations, as shown in figure 2(a) where the flexible shaft is mounted in a free-free condition, in figure 2(b) where a disc of 100 mm thickness is mounted on the shaft, and (c) where two discs of 100 mm and 80 mm thickness are mounted on the flexible shaft. The excitation and measurement nodes along the shaft length are depicted in red in figure 2. Note that only the nodes from 9 to 21 are visible. They are the nodes used to excite lateral transient vibrations of the shaft by impacting the hammer (element 2) at the shaft nodes 1 to 21 and measuring the shaft lateral acceleration responses at the nodes 19 or 10 with the accelerometer (element 1).

2 Modelling the Lateral Dynamics of Flexible Shaft

1. Modelling – In the design phase of a rotating machine, the design engineer will obtain the drawing of the machine elements to simulate the system dynamics. In appendix B, drawings of the flexible shaft are presented.

a) Build a mechanical model to analyze lateral vibrations of the shaft in a free-free condition (without bearings), stating clearly the modeling assumptions and geometrical simplifications used. In other words, when you use a beam, a plate, or a solid element within the Finite Element Method (FEM), some assumptions were made to build the finite elements which you will use in the modeling process. What are the modeling assumptions made to achieve the mass, gyroscopic, and stiffness matrices of the shaft element which you are going to use?

b) Build a correspondent mathematical model using the Finite Element Method. Discretize the flexible shaft using at least 3 different levels of discretization, starting with a very coarse discrete model.

c) Calculate the undamped natural frequencies and modes shapes of shaft in a free-free condition using the MatLab program presented during the lectures *"flexible_rotor_modal_DTU_c.m"*.

d) Carry out a convergence study (table), illustrating how the first 4 undamped natural frequencies associated to the flexible bending modes of the shaft in one single plane (X-Y) or (X-Z) vary depending on the number of shaft elements used. Use at least 3 levels of discretization. Remember that in the low frequency range, you have the rigid body modes with frequencies close to zero. Neglect them in this analysis.

IMPORTANT: *In case you face numerical problems while calculating the system eigenvalues due to zeros associated to rigid body motion, add small values of bearing stiffness at the bearing nodes to overcome the numerical problem. Pay also attention to the length of the shaft elements to avoid numerical "unbalanced" matrices which makes the calculation of eigenvalues and eigenvectors troublesome.*

2. Validation – After simulating the dynamic behaviour of the shaft in a free-free condition, you have the possibility of checking the model accuracy by comparing the theoretical natural frequencies with the experimental ones obtained from an experimental modal analysis test and illustrated in figure 3. Figure 3 depicts three time series and their Fast Fourier Transformation (FFT) obtained when the shaft is excited by the impact hammer at nodes 18, 8, and 4 and its lateral acceleration response is measured using the accelerometer placed at the node 10. Four natural frequencies can be clearly seen in the range of 0 to 3000 Hz,

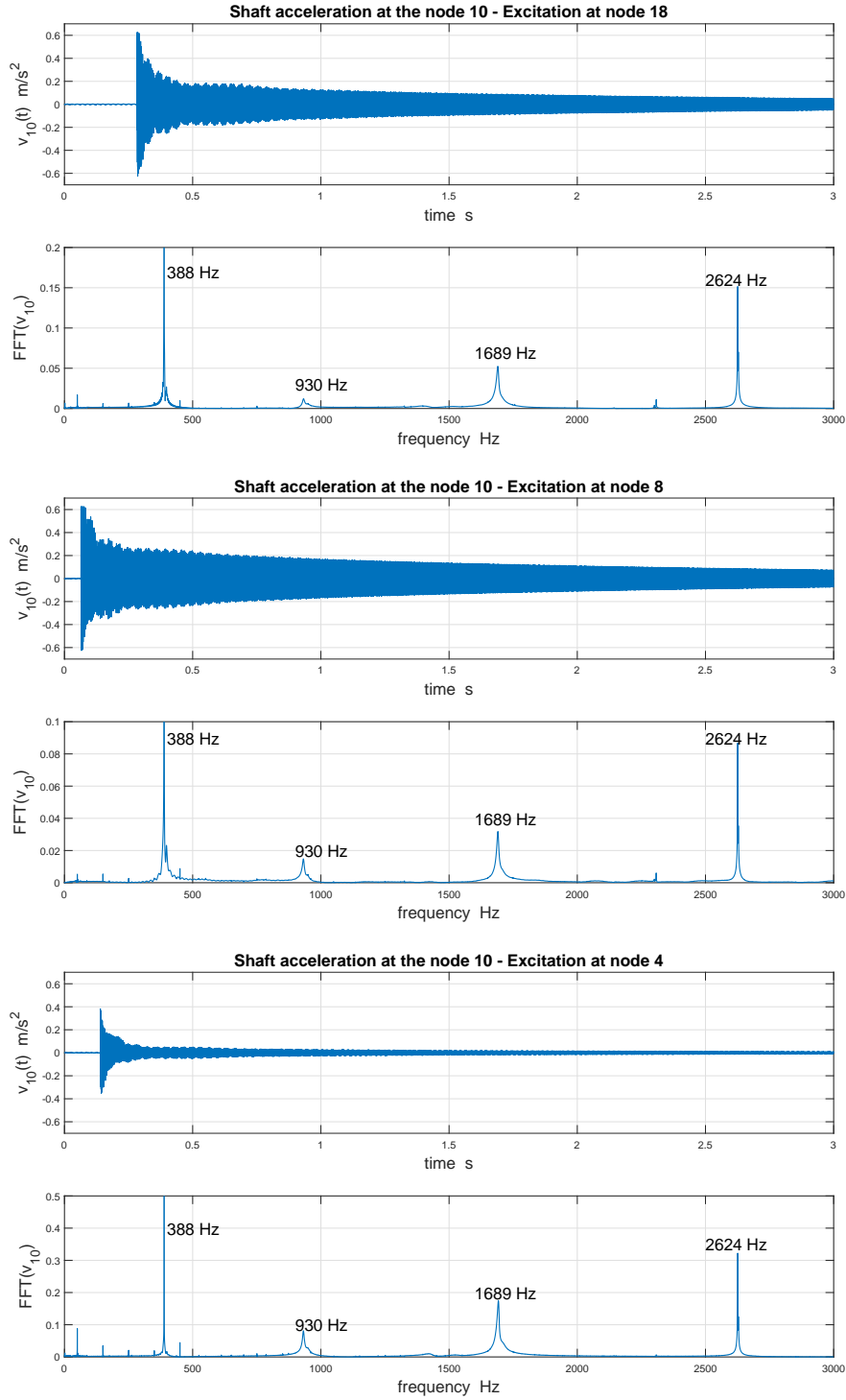


Figure 3: *Partial results of experimental modal testing – flexible shaft in a "free-free" condition and its natural frequencies. Three time series and their Fast Fourier Transformation (FFT) obtained when the shaft is excited by the impact hammer at nodes 18, 8, and 4 and its lateral acceleration response is measured using the accelerometer placed at the node 10.*

namely, 388 Hz, 930 Hz, 1689 Hz, and 2624 Hz. Present the theoretical and experimental results in a form of table and state clearly the discrepancies in %.

3. Model Adjustment - Using the results from the experimental modal analysis (natural frequencies) try to adjust the model parameters having as main goal discrepancies among the theoretical and experimental natural frequencies under 5% in the frequency range of 100 Hz and 3000 Hz. Present the theoretical and experimental results in a form of table and state clearly the discrepancies in %. If you are not able to adjust them under such a precision, try to explain with reasonable argumentation the origin of the discrepancies.

3 Modeling the Lateral Dynamics of Flexible Shaft and Discs

1. Modeling – In appendix B, the drawings of two discs (impellers) are presented.
 - a) Build a mechanical model for the two discs and state the modeling assumptions made to build the disc finite element. Explain the geometrical simplifications made by you to achieve disc parameters of mass and inertia.
 - b) Mount the disc of 100 mm thickness onto the flexible shaft as shown in figure 2(b), build a corresponding mathematical model using the Finite Element Method, and calculate the natural frequencies and modes shapes of the shaft-disc system in a free-free condition, using the MatLab program presented during the lectures "*flexible_rotor_modal_DTU_c.m*".
 - c) Mount the disc of 80 mm thickness – additionally to the disc of 100 mm – onto the flexible shaft as shown in figure 2(c), elaborate a corresponding mathematical model using the Finite Element Method, and calculate the natural frequencies and modes shapes of the shaft-disc system in a free-free condition, using the MatLab program presented during the lectures "*flexible_rotor_modal_DTU_c.m*".
2. Validation – After simulating the dynamic behavior of the shaft and discs in a free-free condition, you have the possibility of checking the model accuracy by comparing the theoretical natural frequencies with the experimental ones obtained from experimental modal testing reported in figures 4 and 5. i) Present the theoretical results for the configuration with one disc, as well as with two discs, and the experimental results in the form of a table and calculate the discrepancies in %. ii) Explain possible discrepancies between theoretical and experimental natural frequencies based on the assumptions made to build the mechanical models and the way how the experiment was set up.
3. Model Adjustment - Using the results from the experimental modal analysis (natural frequencies) try to adjust the model parameters having as main goal discrepancies among the theoretical and experimental natural frequencies under 5% in the frequency range of 100 Hz and 3000 Hz. Present the theoretical and experimental results in a form of table and state the discrepancies in %. If you are not able to adjust them under such a precision, try to explain the reasons for the discrepancies using reasonable argumentation.

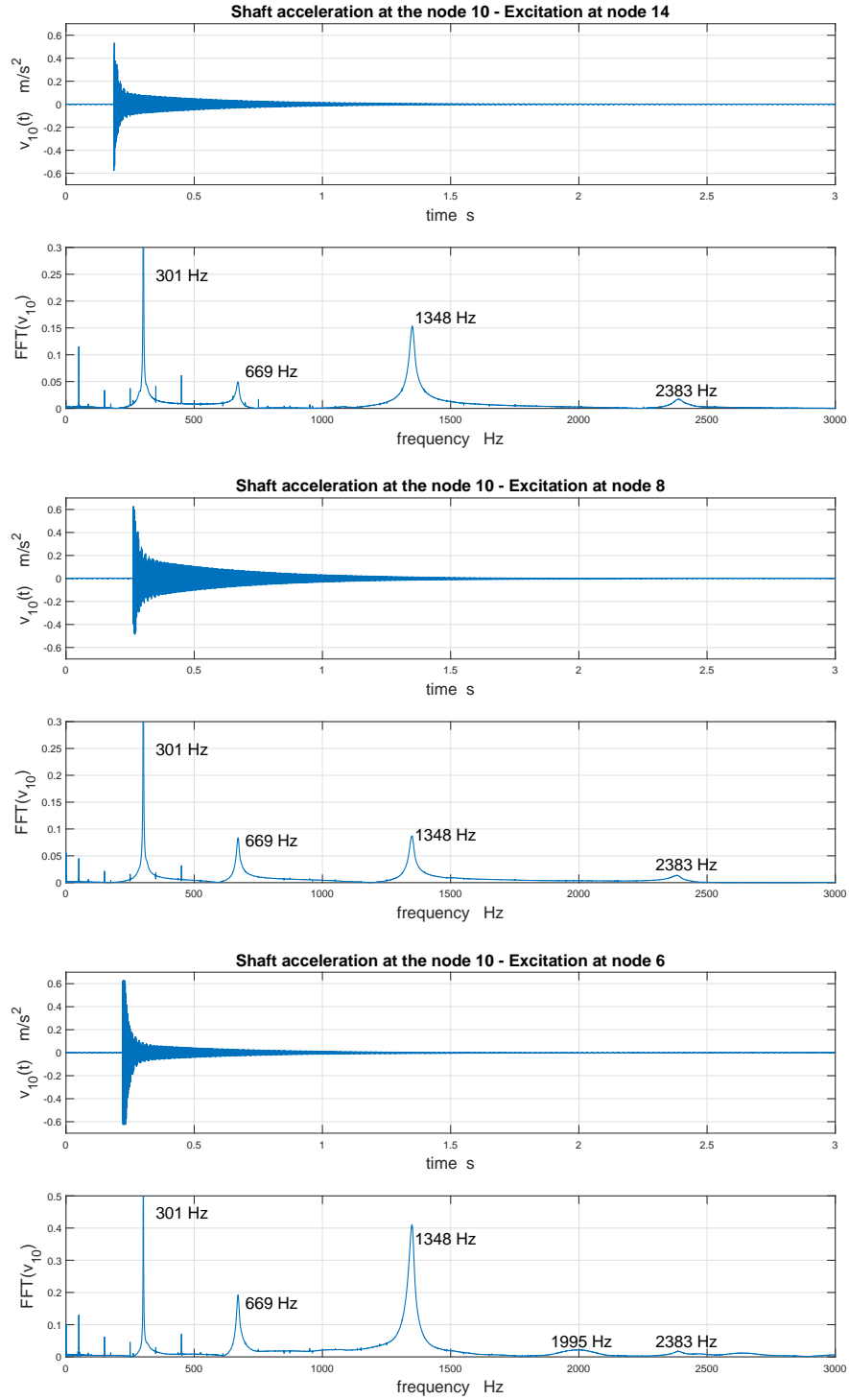


Figure 4: Partial results from experimental modal testing – flexible shaft coupled to the rigid disc of 100 mm thickness in a “free-free” condition and its natural frequencies. Three time series and their Fast Fourier Transformation (FFT) obtained when the shaft is excited by the impact hammer at nodes 14, 8, and 6 and its lateral acceleration response is measured using the accelerometer placed at the node 10.

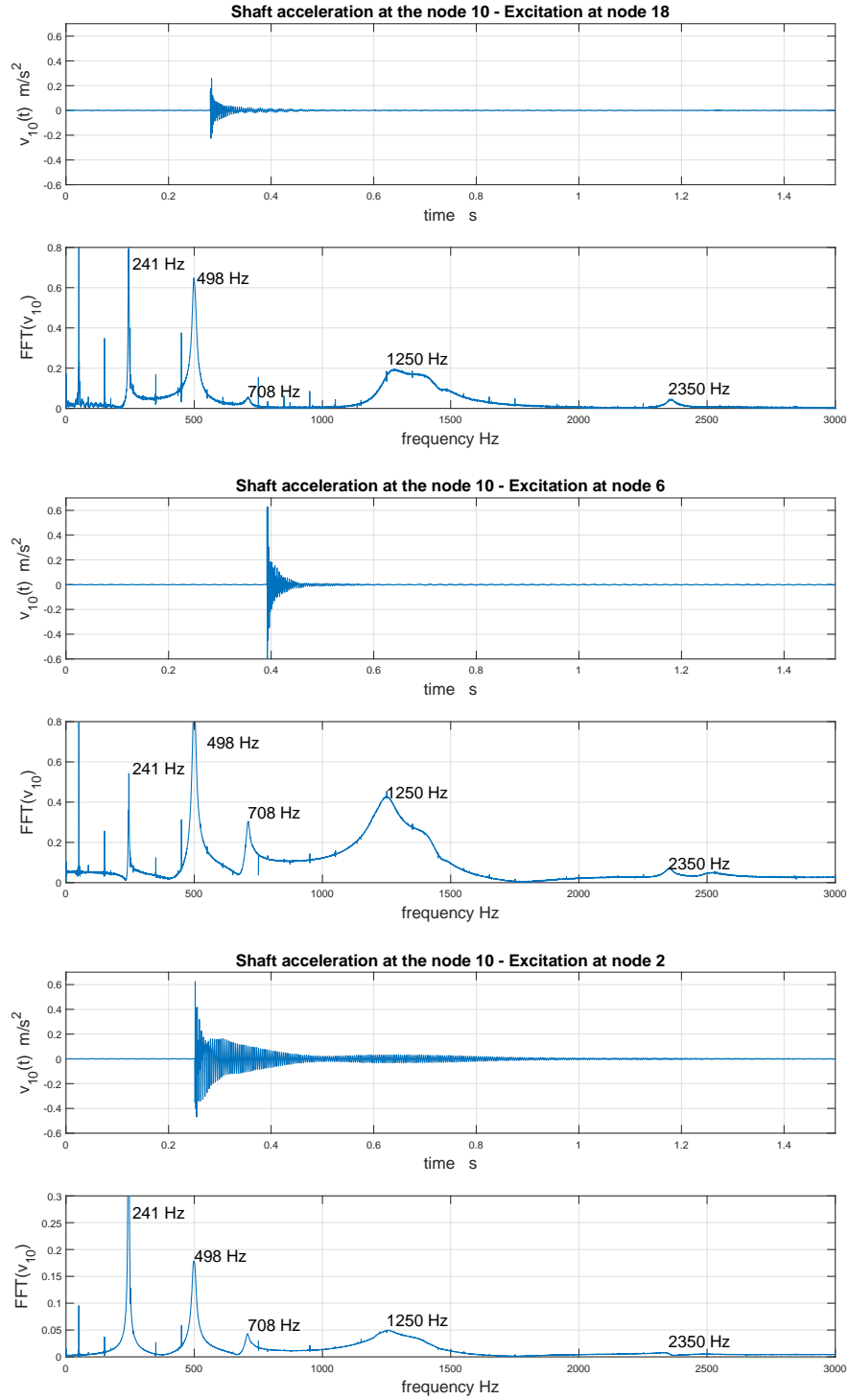


Figure 5: Partial results from experimental modal testing – flexible shaft coupled to the two rigid discs of 100 mm and 80 mm thickness in a “free-free” condition and its natural frequencies. Three time series and their Fast Fourier Transformation (FFT) obtained when the shaft is excited by the impact hammer at nodes 18, 6, and 2 and its lateral acceleration response is measured using the accelerometer placed at the node 10.

4 Modelling the Ball Bearing as Stiffness Element and Coupling to Flexible Shaft and Discs

Three flexible rotating systems, i.e. **system (I)** with only the flexible shaft, **system (II)** with the flexible shaft plus the rigid disc of 100 mm thickness, and **system (III)** with the flexible shaft plus the two rigid discs of 100 mm and 80 mm thickness will now be mounted onto ball bearings located at positions ③ and ⑥ in figure 1(a). The shaft diameters at these locations are 99.6 mm and 50 mm as seen from appendix B. The elasticity of rolling bearings is generally small, even when the loads are high; in most bearing arrangements it is therefore not important. You can assume that its stiffness can be considered of the order 10^9 N/m for practical simulation purposes. If you want to calculate the stiffness of the rolling bearing the specification is given hereby: SKF 2210-2RS1. Normally it is assumed the one rolling element is positioned exactly in the direction of the load. The calculations are therefore concerned only with the effect of the elastic deformations which the loaded rolling elements and raceways undergo at their contact areas. The elasticity changes during rotation of the rolling elements, oscillating between the minimum and maximum values for the cases of load-on-rolling-element and load-between-rolling elements, respectively. These changes, however, are so small that they can be neglected in the calculations. (see reference: Brändlein, J., Eschmann, P., Hasbargen, L. and Weigand, K (1999). "Ball and Roller Bearings –Theory, Design and Application", John Wiley & Sons Ltd., Third Edition, pages 136-142). After this short explanation, and considering zero angular velocity, answer the following questions:

- a) Neglect the rotor angular velocity, i.e. $\Omega = 0$ and investigate the behavior of the first 8 natural frequencies of the rotor-bearing system (I) – considering only one single plane X-Y or X-Z – by varying the two identical bearing stiffness from 10^1 N/m (almost free-free condition) to 10^9 N/m (simply supported on two ball bearings). Illustrate in a log-log scale graphic the behavior of the first 8 natural frequencies of the rotor-bearing system (I) as a function of the bearing stiffness. Do not neglect the first 4 lowest natural frequencies close to zero as you did in sections 2 and 3 of this assignment! In sections 2 and 3 we were only interested in the natural frequencies associated with the bending movements of the three systems!
- b) Explain and illustrate with pictures how the mode shapes of the rotor-bearing system (I) change depending on the bearing stiffness. Neglect the rotor angular velocity, i.e. $\Omega = 0$

4.1 Prediction of Critical Speeds Using Two Ball Bearings

- a) Plot Campbell's diagram for the rotor-bearing systems (I), (II), and (III) in one single graphic and define the first critical speed of the systems (I), (II), and (III). When building the Campbell's diagram, focus the vertical scale of the graphic on the first two natural frequencies! Use the MatLab program *"overhung_rotor_4dof_ccc.m"* as inspiration for building your Matlab code. Analyze the results coming from Campbell's diagram by comparing the differences in natural frequencies among the systems (i), (II), and (III). when the angular velocity is zero. Afterward, analyze the variation of the natural frequencies as a function of the angular velocity from the three systems. What can you conclude?
- b) Plot the first mode shape of the rotor-bearing systems (I), (II) and (III) at their first critical speeds and explain the differences among the three vibration forms. Use the Matlab code which you wrote in sections 2 and 3 of this assignment based on *"flexible_rotor_modal_DTU_c.m"* to answer the question. For being able to see and report the differences among the first mode shapes of systems (I), (II), and (III), it might be necessary to normalize the modes shapes accordantly.

4.2 Unbalance Response Using Two Ball Bearings

Imagine that the rotor-bearing system (III) with two discs has to operate between the two first critical speeds (or resonances) where the vibration level is normally very small. It calls, supercritical rotating machines and there are many of those in the industry. Nevertheless, to operate between the two critical speeds (or resonances), the rotor-bearing system has to cross the first critical speed (or the first resonance). The maximum vibration amplitude at the disc locations shall not exceed $30\text{ }\mu\text{m}$ while crossing the critical speed. Such a condition shall not be violated. A violation of such criteria will cause rubbing between rotating and non-rotating parts of the machine which may lead to catastrophic failure. Assuming that the shaft, as well as the disc of 80 mm thickness, are perfectly balanced and the unbalance only occurs in the rigid disc of 100 mm thickness, what is the maximum unbalance in $[\text{g}\cdot\text{mm}]$ allowed to assure the design specification? Is it possible to meet such a design specification? Explain.

5 Modelling the Hydrodynamic Bearing as Stiffness and Damping Elements and Coupling to Flexible Shaft and Discs

In the following, the ball bearing located at position ③ in figure 1 will be replaced with a journal bearing so that the bearing set-up corresponds to the real test rig, and damping is added to the system. As a designer, you will have to choose among several journal bearings and justify your choice based on three dynamic criteria:

- i) operational range,
- ii) stability margin and
- iii) maximum vibration amplitude due to unbalance.

There are several types of journal bearings with different dynamic properties, as it is presented in the course website (week 11) and in the book "Someya, T. (1989), Journal Bearing Data Book, Springer". Due to the limit of time to carry out this project, you will though calculate i), ii), and iii) for **one of the two journal bearings**, namely, a) two-axial-groove bearing, $L/D = 0.5$ or b) two-lobe bearing, $L/D = 0.5$, $mp = 2/3$. Moreover, you will carry out the analysis only for **system configuration (II)**, i.e., flexible shaft with one rigid disc. The journal bearing data is presented in appendix A of this assignment and can also be downloaded from the course homepage (week 9):

- **Journal Bearing Data** (project 2)
- **Journal Bearing Data** (matlab example)

5.1 Hydrodynamic Bearing – Static and Dynamic Properties

The static equilibrium position, stiffness and damping coefficients of the rotor-bearing system can be obtained with help of the Sommerfeld number $S = \eta * N * L * D / W * (R/C)^2$ and tables presented in the Journal Bearing Data file, if all parameters η , N , L , D , W , R and C are known. Recall that D is the bearing inner diameter in m; L is the bearing width in m; $R = D/2$ is the rotor radius in m; C is the bearing clearance in m; W - external load in N; η - oil viscosity in $\text{N}\cdot\text{s}/\text{m}^2$; N is rotor angular velocity in 1/s or Hz; $\omega = 2 * \pi * N$ is rotor angular velocity in rad/s; $S = \eta * N * L * D / W * (R/C)^2$ is the Sommerfeld number; $\epsilon = e/C$ is eccentricity ratio; Φ is attitude angle; $K_{ij} = (C/W) * k_{ij}$ ($i, j = v, w$) is the dimensionless stiffness coefficients; $C_{ij} = (C * \omega / W) * d_{ij}$ ($i, j = v, w$) is the dimensionless damping coefficients.

The bearings will be lubricated using the *ISO VG 32* oil. Its viscosity can be described by the expression $\eta = 0.0277 * e^{[0.034*(40-T)]}$, η in N.s/m² and T in C. In this initial analysis, the dependency of the oil temperature on the rotor angular velocity will be neglected. Based on experience with other machines with the same size one can assume that the mean temperature T will be 55 C., in other words, the calculations i), ii), and iii) will be led assuming isothermal hydrodynamic lubrication. The maximum angular velocity N_{max} has to be defined, and this is the most important part of the model application. The shaft diameter D can be obtained from the technical drawings. The relationship $R = D/2$ and the bearing clearance $C = 100 \mu\text{m}$ are pre-defined parameters. The relation L/D will be dependent on the bearing type used and is specified in the journal bearing data tables.

1. Before using/applying any kind of theoretical results, i.e. journal bearing data, a good engineer will always try to clearly understand the theoretical assumptions/simplifications made to obtain the theoretical results, in our case the tables. This engineering practice is very important and prevents engineers from using wrong and inappropriate theoretical data, in ranges where the data should not be used. Violation of the theoretical assumptions leads consequently to wrong analysis. In this framework, answer the following questions: what are the main assumptions/simplifications made to obtain the Reynolds equation, which is the foundation for building the journal bearing data?
2. Calculate the external static load due to the weight acting on the journal bearing W in N. For this purpose, please use the geometry of the shaft elements and rigid discs elements. The Sommerfeld number will become a function of the angular speed of the machine N .
3. Using the journal bearing data illustrate graphically the behavior of the oil film thickness in μm as a function of the angular velocity N in Hz for the journal bearing used.
4. a) Plot the values of stiffness coefficients N/m and damping coefficients N/(m/s) as a function of the angular velocity N in Hz for the different types of journal bearings. Remember that the stiffness coefficients k_{ij} given in N/m are calculated as a function of $k_{ij} = (W/C) * K_{ij}$ ($i, j = x, y$), where K_{ij} are the dimensionless stiffness coefficients obtained from the journal bearing data tables. The damping coefficients d_{ij} given in N/(m/s) are calculated as a function of $k_{ij} = W/(C * \omega) * C_{ij}$ ($i, j = x, y$), where C_{ij} are the dimensionless damping coefficients obtained from the journal bearing data tables.
b) Interpolate the behavior of the stiffness and damping coefficients as a function of the angular velocity using linear piecewise functions. Plot the original values of stiffness and damping coefficients used to build the interpolation functions with star symbols and the interpolated functions with continuous lines. Tip: Check out the MatLab function `interp1`.
c) Write some conclusions about the direct stiffness coefficients, cross coupling stiffness coefficients, and direct damping coefficients when the angular velocity N increases.

5.2 Prediction of Critical Speeds

1. Define the two first critical speeds of the rotor-journal bearing system based on Campbell's diagram considering the hydrodynamic bearing type used.
2. The rotor-bearing system has to operate between the two first critical speeds where the vibration level is normally very small. What is the size of such an operational range using the specific hydrodynamic bearing?

5.3 Prediction of Rotor Bearing Stability Limit

1. Based on the stability map of the rotor-bearing system, calculate the maximum angular speed N that the system can operate without instability problems resulting from the interaction with the oil film forces?
2. When the rotor-bearing system becomes unstable, the flexible shaft and discs vibrate laterally with large displacement amplitudes. What is the frequency of such an unstable vibration?
3. Calculate the ratio between the unstable frequency in Hz and the rotor angular velocity Ω in Hz in the stability threshold for the setup.

5.4 Unbalance Response

The maximum vibration amplitude at the disc locations shall not exceed $30\ \mu\text{m}$ along with the whole operational speed range. Such a condition shall not be violated. A violation of such criteria will cause rubbing between rotating and non-rotating parts of the machine and might lead to catastrophic failure. Assuming that the shaft and the disc of 80 mm thickness are perfectly balanced and the unbalance only occurs in the rigid disc of 100 mm thickness, what is the maximum unbalance in $[\text{g}\cdot\text{mm}]$ allowed at the disc of 100 mm to assure the design specification for the rotor-bearing system?

5.5 Engineering Design – Application¹

Rotor-Bearing Design – Change now the ball bearing used by a new hydrodynamic bearing with the same diameter as the ball bearing (see drawing) with a clearance of $C = 85\ [\mu\text{m}]$. What can you conclude about the stability margin of the new rotor-bearing systems operating on two hydrodynamic bearings instead of one ball bearing and one hydrodynamic bearing as originally proposed? Explain.

¹For the students who want to fight for a 12 grade

A Journal Bearing Properties

Table 1a : Two-axial-groove bearing, L/D = 0.5

| S | E | Phi | Q | P | T | Kxx | Kxy | Kyx | Kyy | Bxx | Bxy | Byx | Byy |
|-------------|--------|------|--------|-------|-------|------|------|--------|------|------|------|------|---------|
| Table=[5.96 | 0.0750 | 82.6 | 0.0663 | 1.00 | 111.5 | 1.77 | 13.6 | -13.1 | 2.72 | 27.2 | 2.06 | 2.06 | 14.9 |
| 4.43 | 0.100 | 80.4 | 0.0880 | 0.999 | 83.0 | 1.75 | 10.3 | -9.66 | 2.70 | 20.6 | 2.08 | 2.08 | 11.4 |
| 2.07 | 0.200 | 71.6 | 0.170 | 0.999 | 39.5 | 1.88 | 5.63 | -4.41 | 2.56 | 11.2 | 2.22 | 2.22 | 6.43 |
| 1.24 | 0.300 | 64.1 | 0.243 | 0.997 | 24.4 | 2.07 | 4.27 | -2.56 | 2.34 | 8.50 | 2.32 | 2.32 | 4.73 |
| 0.798 | 0.400 | 57.5 | 0.309 | 0.986 | 16.4 | 2.39 | 3.75 | -1.57 | 2.17 | 7.32 | 2.24 | 2.24 | 3.50 |
| 0.517 | 0.500 | 51.1 | 0.366 | 0.967 | 11.3 | 2.89 | 3.57 | -0.924 | 2.03 | 6.81 | 2.10 | 2.10 | 2.60 |
| 0.323 | 0.600 | 44.7 | 0.416 | 0.939 | 7.75 | 3.65 | 3.62 | -0.427 | 1.92 | 6.81 | 2.08 | 2.08 | 2.06 |
| 0.187 | 0.700 | 38.2 | 0.459 | 0.900 | 5.13 | 4.92 | 3.88 | 0.0235 | 1.83 | 7.32 | 2.16 | 2.16 | 1.70 |
| 0.135 | 0.750 | 34.9 | 0.478 | 0.875 | 4.07 | 5.90 | 4.11 | 0.258 | 1.80 | 7.65 | 2.10 | 2.10 | 1.46 |
| 0.0926 | 0.800 | 31.2 | 0.496 | 0.846 | 3.13 | 7.35 | 4.46 | 0.527 | 1.78 | 8.17 | 2.05 | 2.05 | 1.24 |
| 0.0582 | 0.850 | 27.2 | 0.510 | 0.806 | 2.30 | 9.56 | 4.92 | 0.805 | 1.73 | 9.12 | 2.06 | 2.06 | 1.06 |
| 0.0315 | 0.900 | 22.7 | 0.524 | 0.758 | 1.56 | 13.8 | 5.76 | 1.24 | 1.72 | 10.6 | 2.03 | 2.03 | 0.846 |
| 0.00499 | 0.975 | 12.5 | 0.543 | 0.663 | 0.543 | 43.3 | 9.61 | 4.26 | 1.99 | 22.4 | 2.93 | 2.93 | 0.637]; |

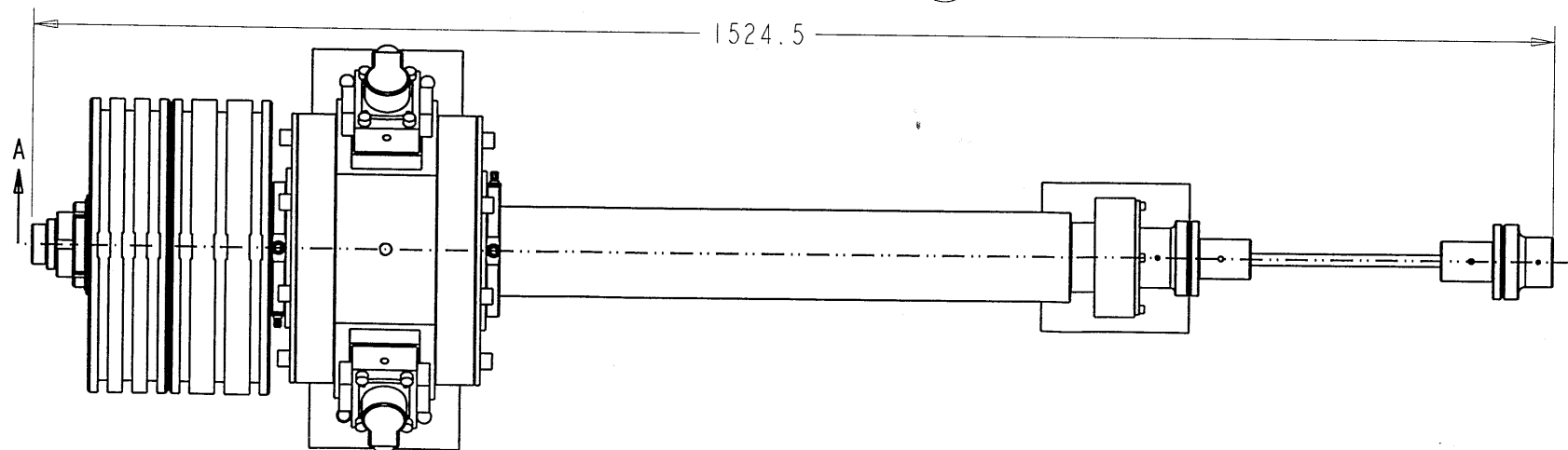
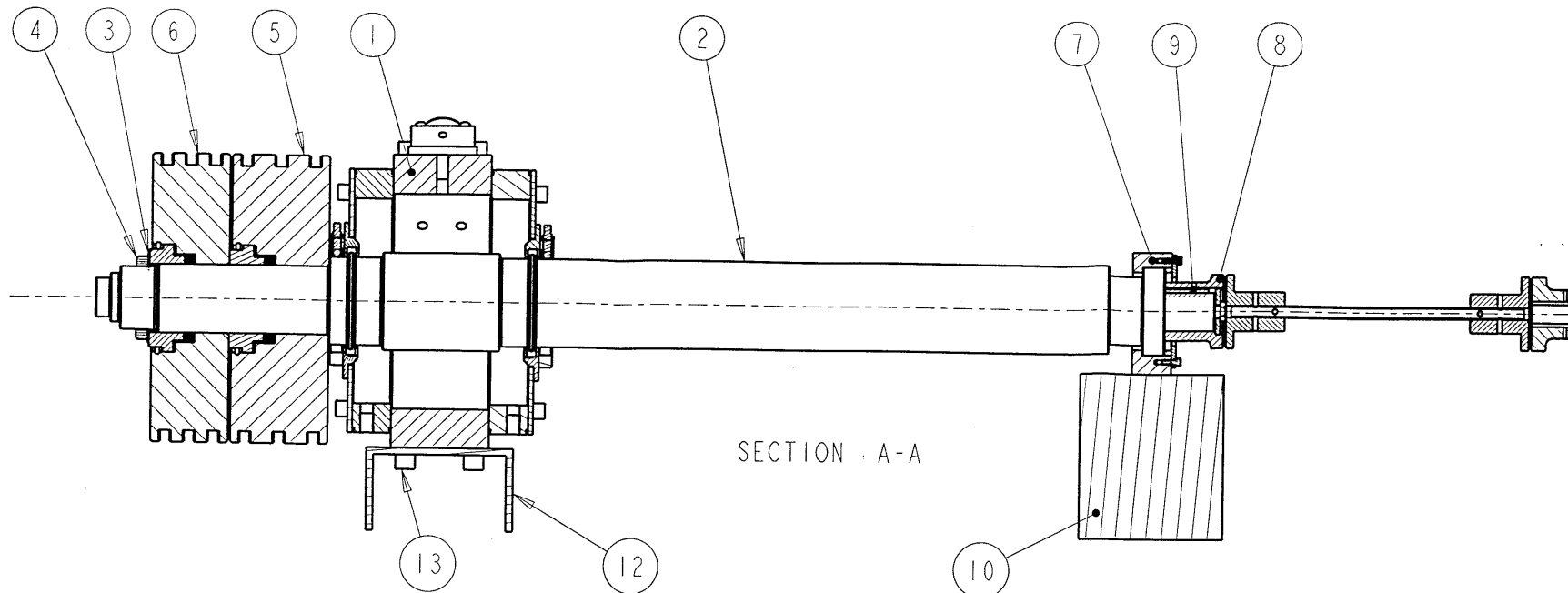
Table 1a : Two-lobe bearing, L/D = 0.5, mp = 2/3

| S | E | Phi | Q | P | T | Kxx | Kxy | Kyx | Kyy | Bxx | Bxy | Byx | Byy |
|-------------|--------|------|-------|-------|-------|------|------|--------|------|------|--------|--------|---------|
| Table=[5.25 | 0.0313 | 79.0 | 0.374 | 0.362 | 135 | 224 | 55.7 | -120 | 23.0 | 314 | -101 | -101 | 66.2 |
| 3.00 | 0.0547 | 79.0 | 0.375 | 0.362 | 76.7 | 129 | 30.2 | -68.6 | 13.2 | 176 | -57.8 | -57.7 | 38.0 |
| 2.02 | 0.0828 | 79.0 | 0.375 | 0.362 | 50.7 | 87.4 | 19.3 | -46.1 | 8.97 | 112 | -38.7 | -38.5 | 25.5 |
| 1.01 | 0.167 | 78.8 | 0.377 | 0.360 | 25.8 | 43.9 | 9.85 | -23.1 | 4.61 | 61.9 | -19.0 | -18.9 | 13.0 |
| 0.515 | 0.317 | 78.3 | 0.381 | 0.354 | 13.2 | 24.0 | 5.29 | -11.8 | 2.60 | 30.2 | -9.42 | -9.38 | 6.86 |
| 0.304 | 0.505 | 77.3 | 0.394 | 0.341 | 8.01 | 15.5 | 4.07 | -6.77 | 1.89 | 19.7 | -5.27 | -5.24 | 4.42 |
| 0.201 | 0.665 | 76.0 | 0.402 | 0.331 | 5.52 | 12.3 | 3.74 | -4.61 | 1.56 | 15.1 | -2.89 | -2.82 | 3.13 |
| 0.0985 | 0.921 | 73.0 | 0.430 | 0.296 | 3.01 | 10.3 | 4.01 | -1.86 | 1.50 | 10.8 | -0.272 | -0.245 | 1.95 |
| 0.0524 | 1.06 | 67.6 | 0.445 | 0.280 | 1.79 | 11.6 | 4.79 | -0.231 | 1.62 | 9.72 | 0.619 | 0.632 | 1.28 |
| 0.0307 | 1.13 | 61.9 | 0.444 | 0.277 | 1.22 | 14.4 | 5.82 | 0.820 | 1.75 | 10.9 | 1.51 | 1.55 | 1.04 |
| 0.0206 | 1.15 | 57.0 | 0.440 | 0.281 | 0.941 | 17.7 | 6.92 | 1.52 | 1.88 | 12.2 | 1.96 | 2.02 | 0.957 |
| 0.0100 | 1.13 | 47.1 | 0.416 | 0.300 | 0.602 | 28.0 | 9.23 | 2.89 | 2.14 | 15.6 | 2.71 | 2.75 | 0.841]; |

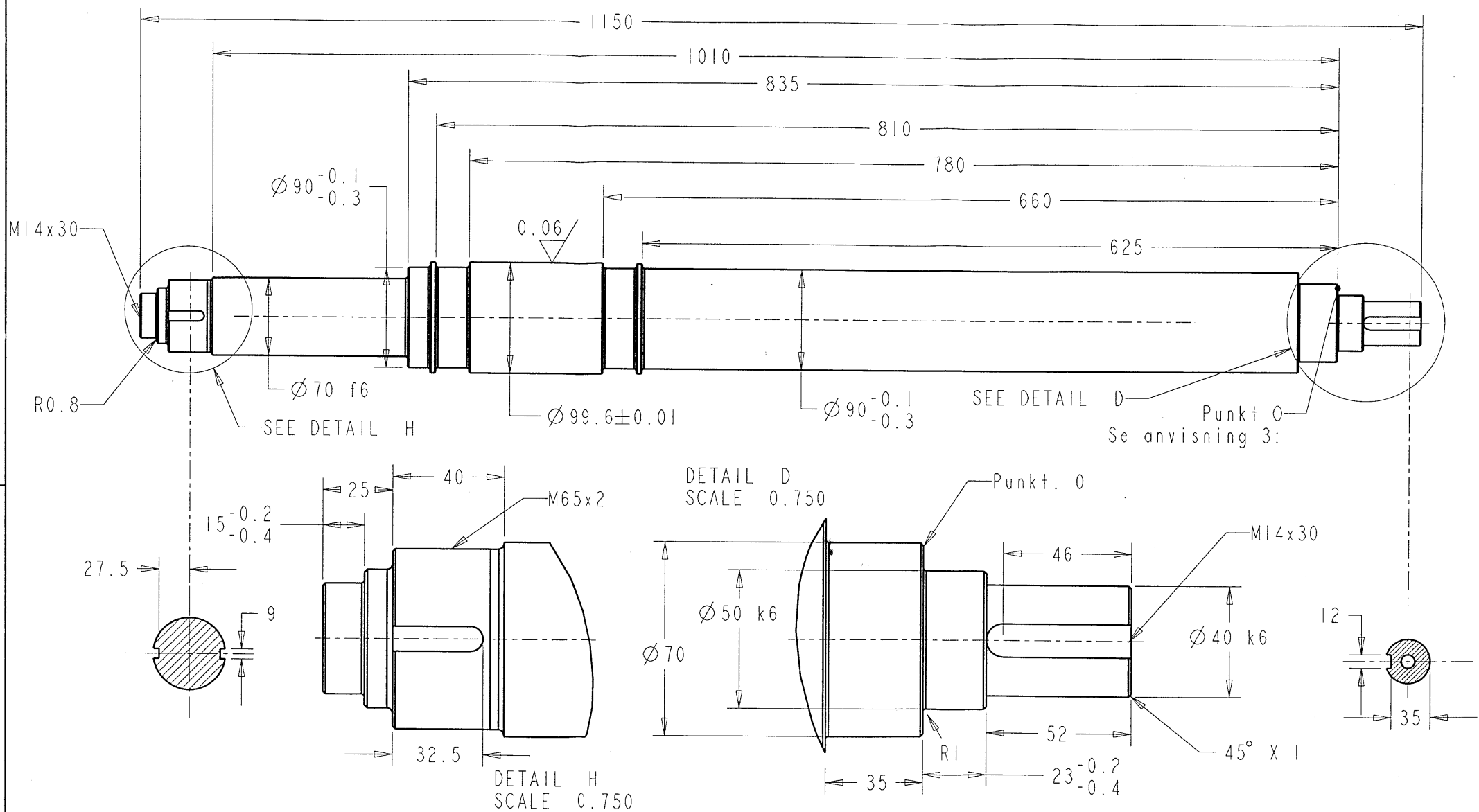
B Technical Drawings of Shaft and Discs

On the following pages you will find technical drawings of:

- Assembly drawing of shaft with two mounted discs.
- Shaft drawing with dimensions.
- Shaft drawing with grinding tolerances.
- 80 mm disc drawing with dimensions.
- 100 mm disc drawing with dimensions.



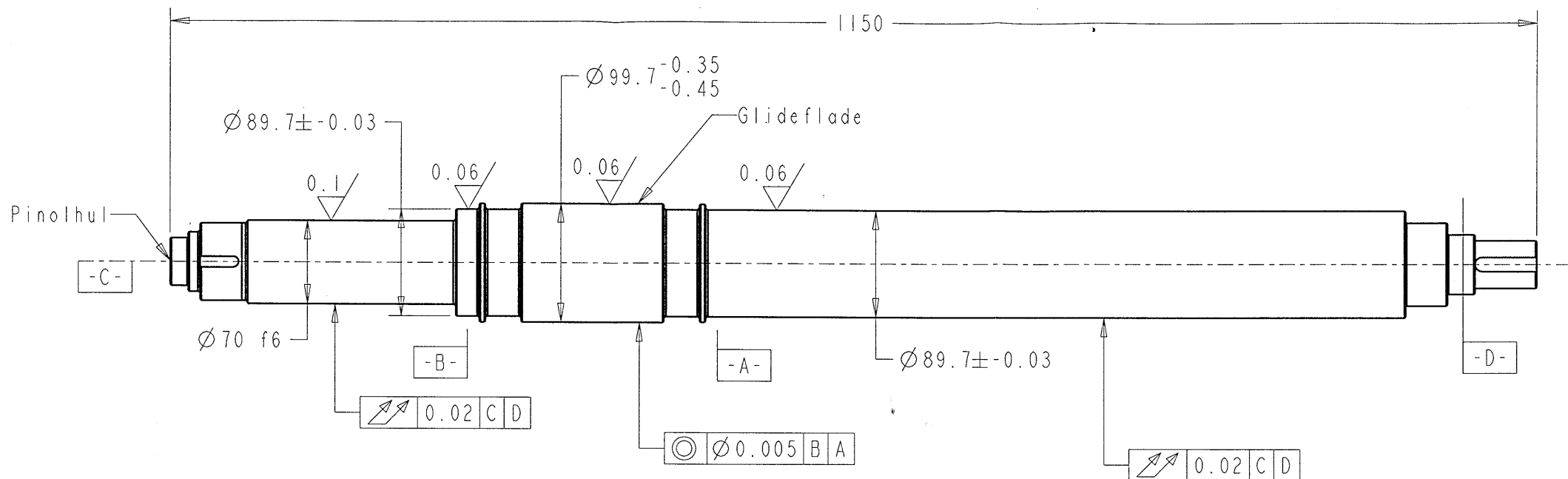
| | |
|----------------------------------|-------------|
| Afgangsprojekt 2001 © Hybridleje | |
| Emne Komplet_opstilling | Antal: |
| teg. Nr. Snit_1-nr | Mat: |
| Kontaktpersoner | |
| Erik Østergaard Tlf. 45256204 | Scale: 0.20 |
| Peder Klit Tlf. 45256267 | Dato: |
| Ilmar Santos Tlf. 45256269 | |



- 1: Alle kanter reifes 45° x 1 mm
- 2: Ved alle overgange i diameter, afrundes brystet med R2 hvis andet ikke er opgivet.
- 3: Alle mål angivet fra punkt 0 sletdrejes i et stykke for at undgå kast.

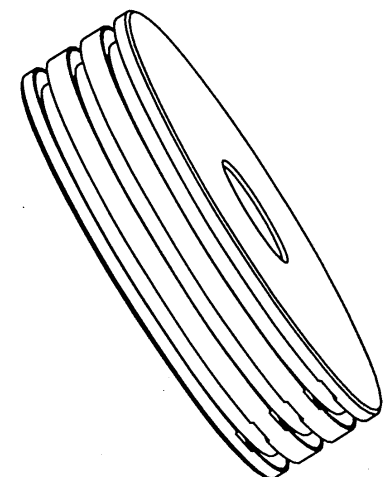
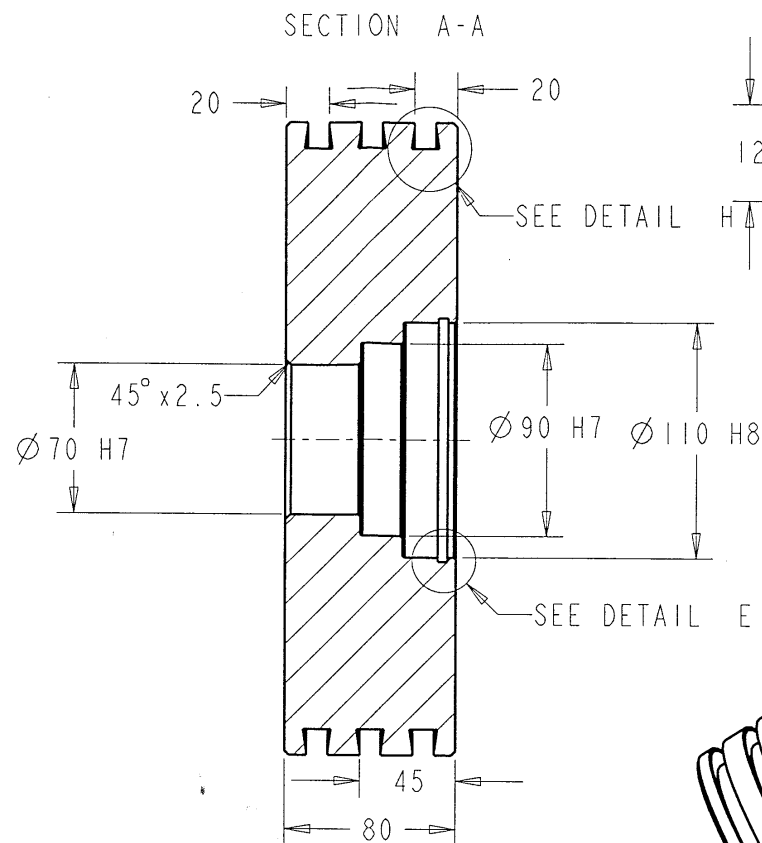
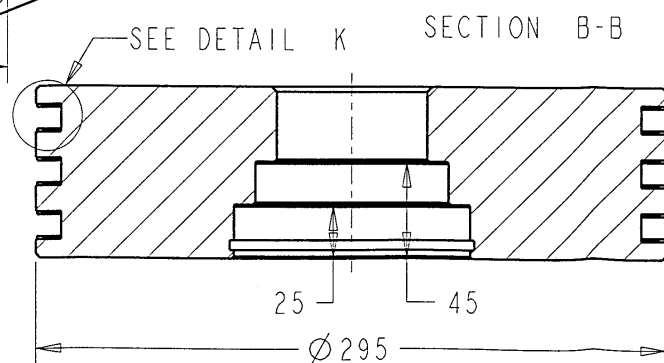
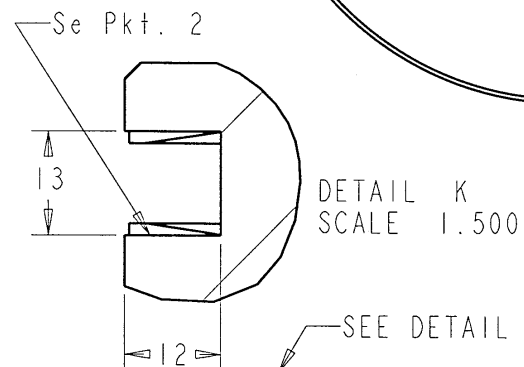
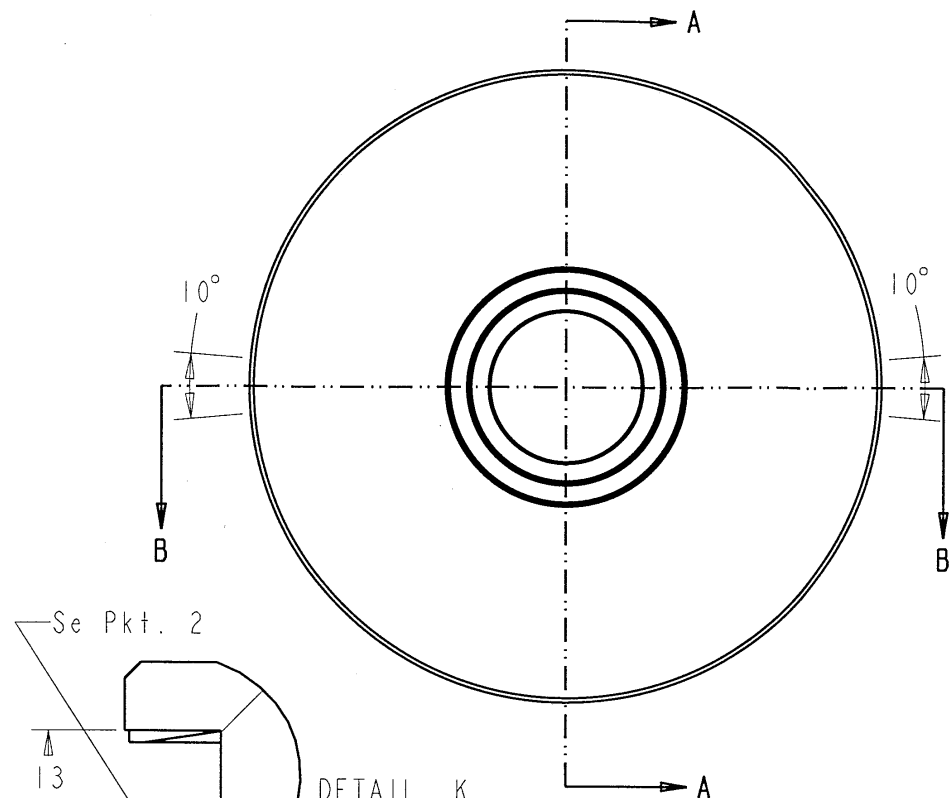
Afgangsprojekt 2001 © Hybridleje

| | | | |
|--|--------------|---------|-------|
| Emne | Hovede_aksel | Antal: | 1 |
| teg. Nr. | 2-1 | Mat:St. | 60-2 |
| Kontaktpersoner Erik Østergaard Tlf. 45256204 Peder Klit Tlf. 45256267 Ilmar Santos Tlf. 45256269 | | Scale: | 0.3 |
| | | Dato: | 10/10 |

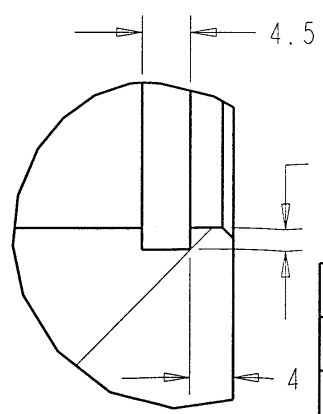


- 1: Totalkast for de slebet flader er 0,02 mm. Eftervisning af totalkast foretages ved at akslen understøttes i punktet D, samt pinolhullet i punktet C.
- 2: Koaksialitet af glideflade i forhold til målefladerne A og B, er 0.005 mm.
- 3: Alle slebne overfladeruheder er angivet som Ra.

| Afgangsprojekt 2001 © Hybridleje | | |
|--|--------------|--------------|
| Emne | Hovede_aksel | Antal: 1 |
| teg. Nr. | 2_1_slib | Mat:St. 60-2 |
| Kontaktpersoner Erik Østergaard Tlf. 45256204 Peder Klit Tlf. 45256267 Ilmar Santos Tlf. 45256269 | | Scale: 0.3 |
| | | Dato: 10/10 |

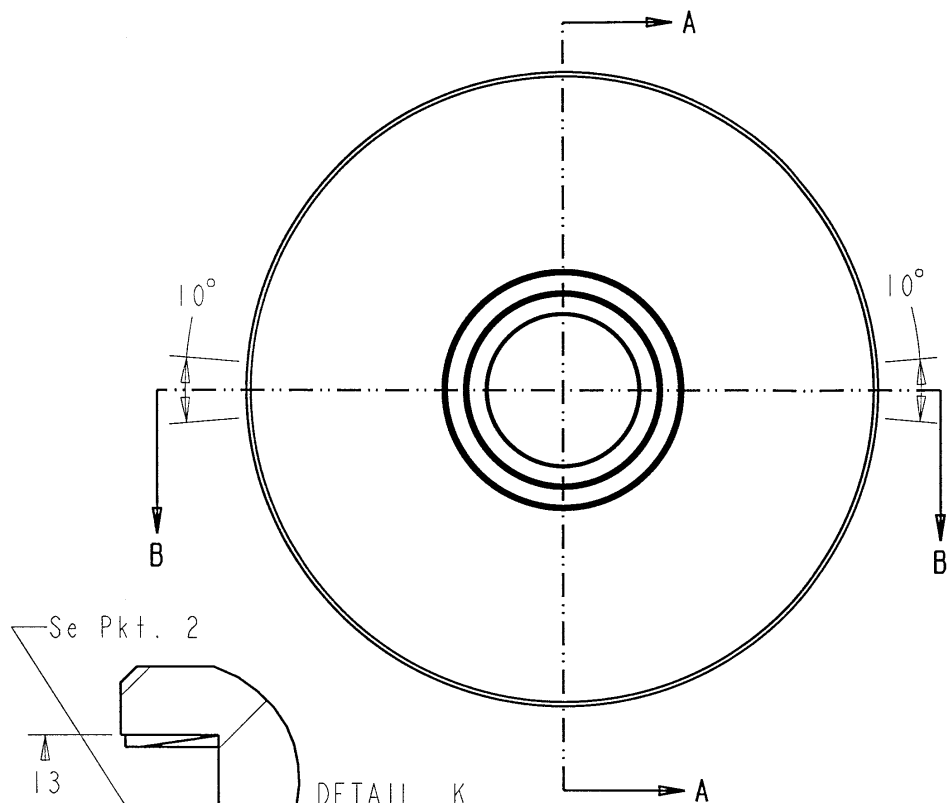


SCALE 0.300

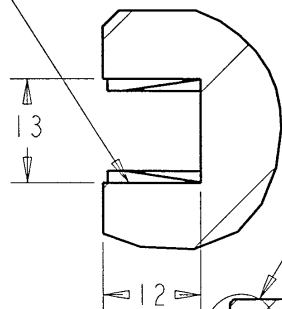


- 1: Alle kanter reifes 45°x0.5 hvis andet ikke er opgivet
 - 2: Åbning i svaegang fræses med Ø10 mm HS.
- Der fræses 2 åbninger i hvert spor som placeres 180 grader forskudt. Hver åbning er 10 grader center til center.

| | | |
|--|--------------|-------------|
| Afgangsprojekt 2001 © Hybridleje | | |
| Emne | svinghjul_80 | Antal: 1 |
| teg. Nr. | 2-6 | Mat: St.60 |
| Kontaktpersoner Erik Østergaard Tlf. 45256204 Peder Klit Tlf. 45256267 Ilmar Santos Tlf. 45256269 | | Scale: 0.4 |
| | | Dato: 10/10 |
| | | |



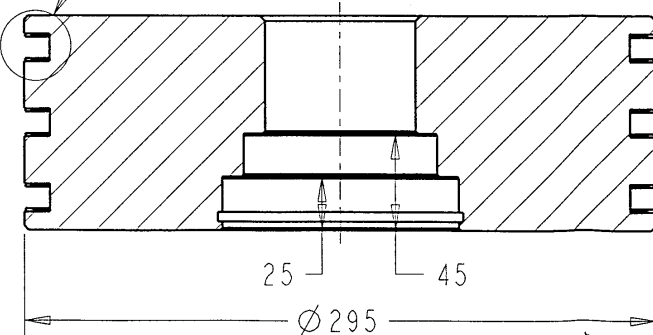
Se Pkt. 2



DETAIL K
SCALE 1.500

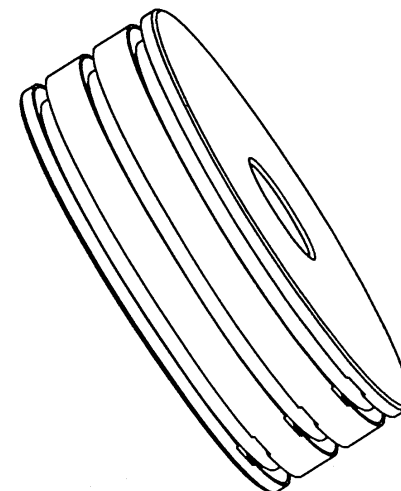
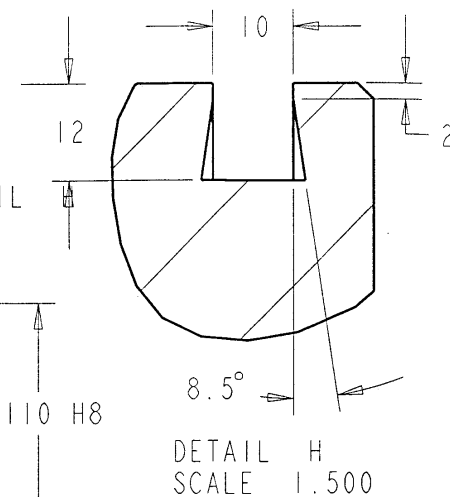
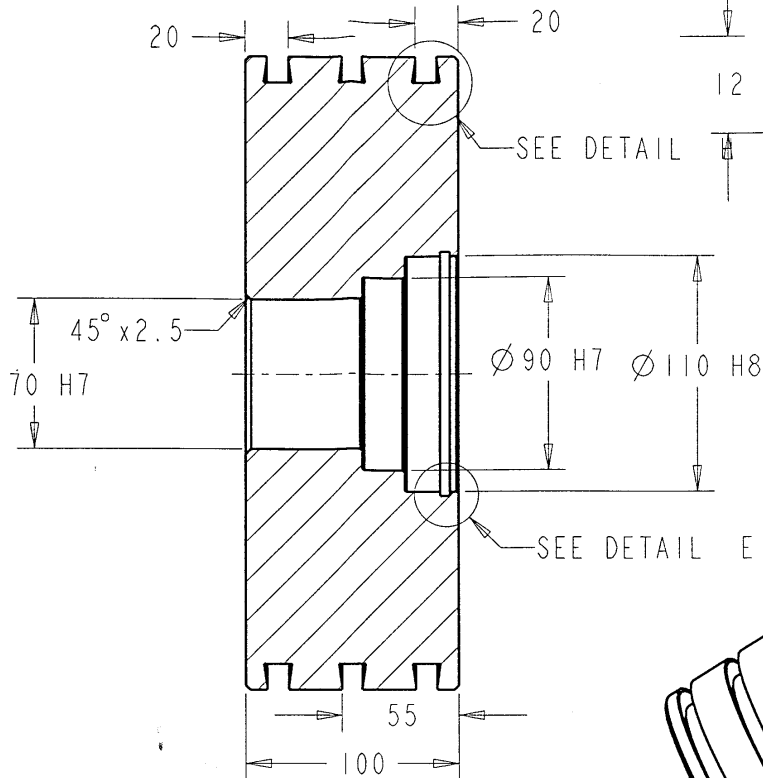
SEE DETAIL K

SECTION B-B

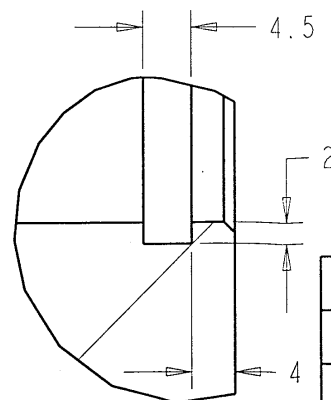


- 1: Alle kanter reifes $45^\circ \times 0.5$ hvis andet ikke er opgivet
 2: Åbning i sylegang fræses med $\varnothing 10$ mm HS.
 Der fræses 2 åbninger i hvert spor som placeres 180 grader forskudt. Hver åbning er 10 grader center til center.

SECTION A-A



SCALE 0.300



DETAIL E
SCALE 2.000

Afgangsprojekt 2001 © Hybridleje

Emne svinghjul_100

Antal: 1

teg. Nr. 2-5

Mat: St.60

Kontaktpersoner

Erik Østergaard Tlf. 45256204
 Peder Klit Tlf. 45256267
 Ilmar Santos Tlf. 45256269

Scale: 0.4

Dato: 10/10